Voltage Sag Planning of Industry Power System Using Hybrid Differential Evolution Considering CBEMA Curve

Yao-Hung Chan, Chi-Jui Wu, Wei-Neng Chang, and Ying-Pin Chang

Abstract—This paper is used to investigate the voltage sag planning of a radial industrial power system using the hybrid differential evolution (HDE) method. The analysis considers the CBEMA curve and coordination of over-current relays. Firstly, the analytical equations for direct calculation of voltage sag are investigated to obtain the sag severity of the system after single or three-phase faults. The equations are useful in the planning procedures using HDE. Then, the effect of over-current relay setting on the sag duration is evaluated. Finally, the HDE is used to obtain the impedance values of transformers considering the CBEMA curves. The relay time multiplier factor is also a variable. The test on a radial industrial power system with three △/Y-g connected transformers is chosen to reveal the effectiveness of this method. The study results show that the voltage sag severity can be controlled by the structure of the power system, the transformer impedances, and the relay setting.

Keywords—Voltage sag, over-current relay, power quality, CBEMA curve, hybrid differential evolution method.

I. INTRODUCTION

Voltage sag is one of indexes of power quality degradation. Some momentary events cause drop of voltage during the transient period until protective relay are activated, and the circuit breaker is used to clean the faults. Possible and inevitable causes of faults in power systems include grounding faults, poor insulation of equipment, or transmission line faults caused by animals or other objects. For example, the power system transmission line is suddenly struck by lightning. When voltage sag occurs, the voltage values may fall into 10% to 90% of the normal value in a period of is 0.5 cycle to a few seconds [1-2].

The voltage sag magnitude and duration are the essential characteristics. It comprises two parts: the drop in the voltage (ΔV) [3-11] and the duration (Δt) [12-13]. ΔV is determined by the system impedances and fault types, and Δt is determined by the protective relay and the action of the circuit breaker. This phenomenon can be expressed as the rectangular area in Fig. 1. It can define the voltage sag severity as $\Delta V \times \Delta t$. Relevant limits on acceptable voltage sag are defined for both consumer

electronic products, large electrical equipments, and semiconductor manufacturing machines. They can be divided roughly into static load and dynamic load. With respect to the static load, the CBEMA (Computer Business Equipment Manufacturers Association) has suggested the voltage curve as plotted in Fig. 2 [14-18] for computer equipments. Additionally, SEMI (Semiconductor Equipment and Materials International) also has developed the SEMI curve to define the transition ability of semiconductor devices during voltage sag.

In this paper, the optimal voltage sag planning by the method of HDE (hybrid differential evolution method), which is a direct and parallel search method that involves accelerating and migrant operations is used to prevent falling into local optimal solutions [19-25]. This optimization method enables to determine system equipment parameters over a range. Power systems can be optimized using the CBEMA voltage curve and protective coordination to set the parameters of the system equipment. The transformer impedance and time multiplier of protective relay are variables. The simulation results show the proposed method can obtain the optimal solutions while the voltage sag conditions satisfy the CMEMA curve.
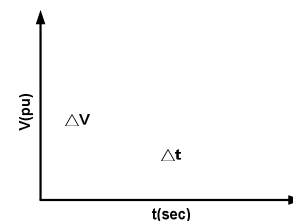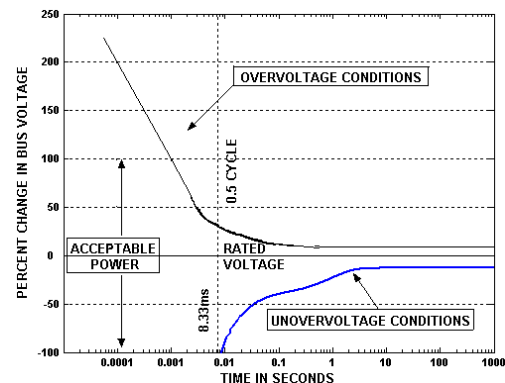

Fig. 1. Voltage sag characteristics.

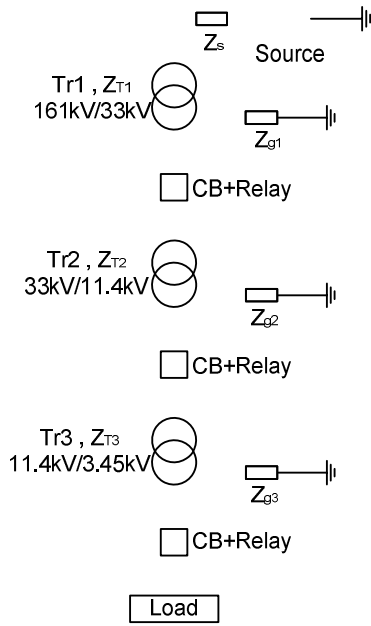

Fig. 2. CBEMA power acceptability curve [15, 16, 18].

Fig. 3. A radial industrial power system with four voltage levels and △/Y-g connected transformers.
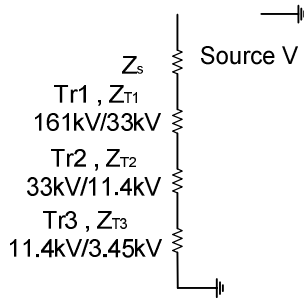

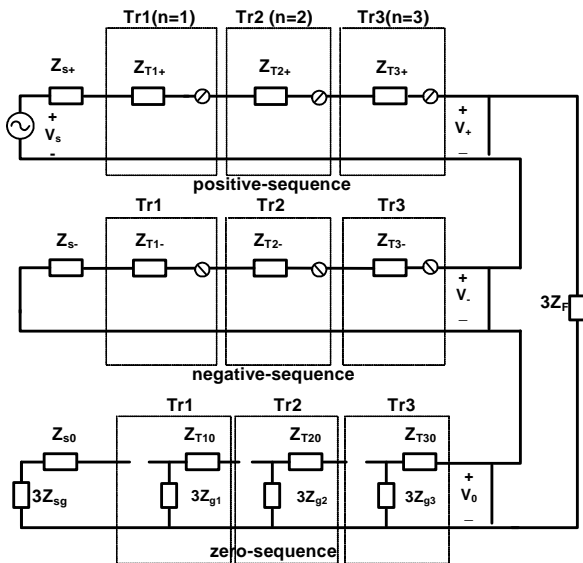Fig. 4. Equivalent sequence network of three-line-ground fault (3LG) analysis at 3.45-kV bus.

Fig. 5. Equivalent sequence network for single-line-ground fault (SLG) analysis at 3.45-kV bus.

II. EQUATIONS FOR DIRECT FAULT CURRENT AND VOLTAGE SAG CALCULATION

The simplified model of the industrial power system under study is displayed in Fig. 3. The voltage source is assumed to be three-phase balanced in Y-ground connection. The three transformers are in △/Y-grounded connection. Four voltage levels, that is, 161-kV, 33-kV, 11.4-kV, and 3.45-kV, are used. In this study, the resistances of transformers are negligible, so that only reactance is used in the calculation of sag severity. To simplify the computation, assume that the positive-, negative-, and zero-sequences impedance are equal.

(a) Three-phase balanced fault: Three-line-grounded fault (3LG)

Firstly, voltage sag and current are derived when a three line-grounded fault occurs at the 3.45-kV bus, as displayed in Fig. 4. Then, the 3.45-kV side fault current and voltage are given by

$$I_{F,3.45} = I_{F,11.4} = I_{F,33} = \frac{1}{\sum X_T} V \tag{1}$$

$$V_{a,3.45} = V_{b,3.45} = V_{c,3.45} = 0 \tag{2}$$

Where X_T is the total reactance of transformers and lines. The bus voltages of the other levels are given by

$$V_{a,161} = V_{b,161} = V_{c,161} = \frac{X_{T1} + X_{T2} + X_{T3}}{\sum X_T} V$$

$$V_{a,33} = V_{b,33} = V_{c,33} = \frac{X_{T2} + X_{T3}}{\sum X_T} V \tag{3}$$

$$V_{a,11.4} = V_{b,11.4} = V_{c,11.4} = \frac{X_{T3}}{\sum X_T} V$$

(b) Single-phase unbalanced fault: Single-line-grounded fault (SLG)

The single-line-grounded fault is a non-symmetric fault, and can be analyzed by using the positive-, negative-, and zero-sequence networks, as displayed in Fig. 5. Suppose that a grounded fault on phase a occurs at the 3.45-kV bus. If the fault is completely grounded, then $Z_F = 0$. The fault currents and voltages at the 3.45-kV level are given by

$$I_{F,3.45} = \frac{3}{2\left(\sum jX_T\right) + \left(jX_{T3} + 3R_{g3}\right)} V_a \tag{4}$$

$$V_{a,3.45} = 0$$

$$V_{b,3.45} = \frac{-j\sqrt{3}\left(\sum jX_T\right) + \left(\frac{-3 - j\sqrt{3}}{2}\right)\left(jX_{T3} + 3R_{g3}\right)}{2\left(\sum jX_T\right) + \left(jX_{T3} + 3R_{g3}\right)} V_a \tag{5}$$

$$V_{c,3.45} = \frac{j\sqrt{3}\left(\sum jX_T\right) + \left(\frac{-3 + j\sqrt{3}}{2}\right)\left(jX_{T3} + 3R_{g3}\right)}{2\left(\sum jX_T\right) + \left(jX_{T3} + 3R_{g3}\right)} V_a$$

Since the transformers are in △/Y-g connection, the 11.4-kV bus does not have zero-sequence current. The fault currents and voltages of the 11.4-kV bus are obtained by

$$I_{a,11.4} = \frac{\sqrt{3}}{2\left(\sum jX_T\right) + \left(jX_{T3} + 3R_{g3}\right)} V_a$$

$$I_{b,11.4} = \frac{-\sqrt{3}}{2\left(\sum jX_T\right) + \left(jX_{T3} + 3R_{g3}\right)} V_a \tag{6}$$

$$I_{c,11.4} = 0$$

$$V_{a,11.4} = \frac{-j\left(\sum jX_T\right)+\left(\frac{\sqrt{3}-j}{2}\right)\left(jX_{T3}+3R_{g3}\right)+\sqrt{3}\left(jX_{T3}\right)}{2\left(\sum jX_T\right)+\left(jX_{T3}+3R_{g3}\right)}V_a$$

$$V_{b,11.4} = \frac{j\left(\sum jX_T\right)+\left(\frac{\sqrt{3}+j}{2}\right)\left(jX_{T3}+3R_{g3}\right)+\sqrt{3}\left(jX_{T3}\right)}{2\left(\sum jX_T\right)+\left(jX_{T3}+3R_{g3}\right)}V_a \quad (7)$$

$$V_{c,11.4} = \frac{2j\left(\sum jX_T\right)+j\left(jX_{T3}+3R_{g3}\right)}{2\left(\sum jX_T\right)+\left(jX_{T3}+3R_{g3}\right)}V_a$$

Similarly, the fault currents and voltages of the 33-kV level are given by

$$I_{a,33} = \frac{1}{2\left(\sum jX_T\right)+\left(jX_{T3}+3R_{g3}\right)}V_a$$

$$I_{b,33} = \frac{-2}{2\left(\sum jX_T\right)+\left(jX_{T3}+3R_{G3}\right)}V_a \quad (8)$$

$$I_{c,33} = \frac{1}{2\left(\sum jX_T\right)+\left(jX_{T3}+3R_{g3}\right)}V_a$$

$$V_{a,33} = \frac{-j\sqrt{3}\left(jX_T\right)+\left(\frac{1-j\sqrt{3}}{2}\right)\left(jX_{T3}+3R_{g3}\right)+jX_{T3}+jX_{T2}}{2\left(\sum jX_T\right)+\left(jX_{T3}+3R_{g3}\right)}V_a \quad (9)$$

$$V_{b,33} = -\frac{\left(jX_{T3}+3R_{g3}\right)+2\left(jX_{T3}\right)+2\left(jX_{T2}\right)}{2\left(\sum jX_T\right)+\left(jX_{T3}+3R_{g3}\right)}V_a$$

$$V_{c,33} = \frac{j\sqrt{3}\left(\sum jX_T\right)+\left(\frac{1+\sqrt{3}}{2}\right)\left(jX_{T3}+3R_{g3}\right)+jX_{T3}+jX_{T2}}{2\left(\sum jX_T\right)+\left(jX_{T3}+3R_{g3}\right)}V_a$$

And that of the 161-kV level are

$$I_{a,161} = 0$$

$$I_{b,161} = \frac{-\sqrt{3}}{2\left(\sum jX_T\right)+\left(jX_{T3}+3R_{g3}\right)}V_a \quad (10)$$

$$I_{c,161} = \frac{\sqrt{3}}{2\left(\sum jX_T\right)+\left(jX_{T3}+3R_{g3}\right)}V_a$$

$$V_{a,161} = \frac{-2j\left(\sum jX_T\right)-j\left(jX_{T3}+3R_{g3}\right)}{2\left(\sum jX_T\right)+\left(jX_{T3}+3R_{g3}\right)}V$$

$$V_{b,161} = \frac{j\left(\sum jX_T\right)+\left(\frac{-\sqrt{3}+j}{2}\right)\left(jX_{T3}+3R_{g3}\right)}{2\left(\sum jX_T\right)+\left(jX_{T3}+3R_{g3}\right)}V$$
$$-\frac{\sqrt{3}\left(jX_{T3}+jX_{T2}+jX_{T1}\right)}{2\left(\sum jX_T\right)+\left(jX_{T3}+3R_{g3}\right)}V \quad (11)$$

$$V_{c,161} = \frac{j\left(\sum jX_T\right)+\left(\frac{\sqrt{3}+j}{2}\right)\left(jX_{T3}+3R_{g3}\right)}{2\left(\sum jX_T\right)+\left(jX_{T3}+3R_{g3}\right)}V$$
$$+\frac{\sqrt{3}\left(jX_{T3}+jX_{T2}+jX_{T1}\right)}{2\left(\sum jX_T\right)+\left(jX_{T3}+3R_{g3}\right)}V$$

III. EFFECT OF OVER-CURRENT RELAY

The voltage sag duration depends on the fault clearing time during which the protective relay and the circuit breaker (CB) operate. The relay considered is only the over-current relay (50/51). The operation time of the relay is obtained from the movement curve. The operation time of the circuit breaker is related to the mechanical characteristic and can be regarded as having a definite value. The duration of voltage sag can be expressed as

$$\Delta t = t_{Ry} + t_{CB} \quad (12)$$

where t_{Ry}: protective relay operating time.
t_{CB}: circuit breaker operating time.
In practical distribution systems, t_{CB} is from 3 cycles to 8 cycles [3].

According to the IEC 60255-22 standard [26], the over-current relay (51) inverse t-I curves are given in (13). The α and β values in TABLE I determine the slopes.

$$t_{Ry}(s) = \frac{k \times \beta}{\left(\frac{I}{I_P}\right)^{\alpha} - 1} \quad (13)$$

Where k: time multiplier
I: current detected by relay (normally the effective value), $I > I_P$
I_P : current setting threshold

If the normal inverse curve relay movement characteristic is chosen, then α=0.02 and β=0.14 can be substituted into (13) to yield the voltage sag duration formulation. Then the $\Delta V_{(F)} \Delta t_{(F)}$ value of voltage sag characteristics can be used to describe the voltage sag range where $\Delta V_{(F)}$ is the drop of voltage, and $\Delta t_{(F)}$ is the duration.

TABLE I
INVERSE T-I CURVE PARAMETERS OF OVER-CURRENT RELAY

	t-I curve setting	α	β
A	Normal Inverse	0.02	0.14
B	Very Inverse	1.0	13.5
C	Extremely Inverse	2.0	80.0
D	Long-Time Inverse	1.0	120.0

TABLE II
SYSTEM DATA

Power Source	Three-phase balanced, 161-kV, Y-connected, $X_{gs} = 0$ Ω, MVA_{sc}=2000 MVA.
Transformer	T_{r1} ： 161/33-kV, 100 MVA, X_{T1}=12 %, △/Y-g connected, Z_{g1}= 20 Ω.
	T_{r2} ： 33/11.4-kV, 20 MVA, X_{T2} =10 %, △/Y-g connected, Z_{g2} = 6 Ω.
	T_{r3} ： 11.4/3.45-kV, 7.5 MVA, X_{T3}=6 %, △/Y-g connected, Z_{g3} = 0 Ω.
Circuit Breaker	T_{CB} = 0.08s

TABLE III
INITIAL SETTING OF PROTECTIVE RELAY INVERSE T-I CURVE

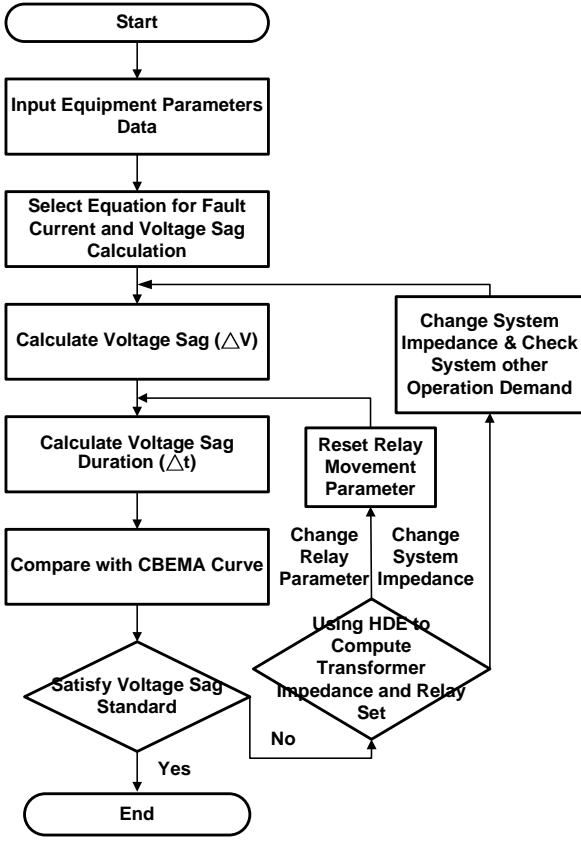| Voltage level	Time multiple (k)
3.45 kV	0.1
11.4 kV	0.2
33 kV	0.3

Fig. 6. Voltage sag analyses flowchart.

(1) three-phase fault：

From Fig. 4, it can be obtained the voltage drop at the 3.45-kV level.

$$\Delta V_{(F)} = \left(1 - \frac{Z_f}{Z_T + Z_f}\right)V$$

If $I_F \geqq I_p$, then

$$\Delta t_{(F)} = \frac{k \times 0.14}{\left|\left(\dfrac{\left(\dfrac{V}{Z_T + Z_f}\right)}{I_P}\right)\right|^{0.02} - 1} + t_{CB} \qquad (14)$$

(2) single line-ground fault：

From Fig. 5, it can be obtained that

$$\Delta V_{(F)} = \left(1 - \frac{Z_{f+} + Z_{f-} + Z_{f0}}{(Z_{f+} + Z_{f-} + Z_{f0}) + (Z_{T+} + Z_{T-} + Z_{T0})}\right)$$

If $I_F \geqq I_p$, then

$$\Delta t_{(F)} = \frac{k \times 0.14}{\left|\dfrac{3V}{\dfrac{(Z_{T+} + Z_{T-} + Z_{T0}) + 3(Z_{f+} + Z_{f-} + Z_{f0})}{I_P}}\right|^{0.02} - 1} + t_{CB} \qquad (15)$$

IV. VOLTAGE SAG ANALYSIS PROCEDURE AND PROBLEM FORMULATION

Figure 6 shows the flowchart for analyzing voltage sag. It is described as follows.

(1) System equipment impedances are transformed to pu values.

(2) Fault currents at all voltage levels are calculated, and the ranges of voltage sag ΔV are obtained.

(3) Choose the curve of over-current relay (50/51). The relay operating time and the circuit breaker operating time are added to yield the fault clearing time, which is also the voltage sag duration Δt.

(4) Compare ΔV and Δt with the CBEMA curve.

The optimization problem is formulated as follows.

(1) Objective function：

$$\text{Minimize } M = \sum \left|V_{unacceptable-point} - V_{CBEMA-curve}\right| \qquad (16)$$

$$\text{Variable vector} = \begin{bmatrix} X_{T1} & X_{T2} & X_{T3} & k_3 \end{bmatrix}^t$$
$$k_3^{min} < k_3 < k_3^{max}$$
$$X_{Ti}^{min} < X_{Ti} < X_{Ti}^{max} \qquad i = 1,2,3 \qquad (17)$$

where k_i：protective relay time multiple at the 3.45kV level.

X_{Tri}：transformer impedance.

(2) Constraint：

(a) equipment parameter: the system equipment parameter's limitation conditions.

(b) voltage regulator rate: The voltage regulation must be limited less than 5%.

$$-5\% < VR_i < 5\% \qquad i = 1,2,3 \qquad (18)$$

(c) coordination of protective relay: The trip time of downstream relay must be less than upstream relay.

$$T_{F,3.45kV} < T_{F,11.4kV} < T_{F,33kV} \qquad (19)$$

V. SIMULATION RESULTS

(a)Three-phase fault

TABLE IV shows the voltage sag results of the system with the original setting. Fig. 7 compares the voltage sag with the CBEMA curve for a three-phase fault of the system with the original setting. It can be found that the 161-kV and 33-kV bus voltage sags are in the CBEMA acceptable region, but the 11.4-kV bus voltage is in the unacceptable region.

Because the fault occurs at the 3.45-kV bus, so we can adjusted the transformer impedances and the 3.45-kV protective relay k value using the HDE method.

Case 1：The transformer impedance is constant and the relay k value is adjusted.

Case 2：The transformer impedance is adjusted and the relay k value is constant.

Case 3：The transformer impedance and the relay k value are adjusted.

TABLE V presents the limitations of the system. TABLE VI and TABLE VII show the calculated results of three cases. They are compared with the CBEMA curve as plotted in Figure 8. Only case 3 is in the acceptable region.

TABLE IV
SIMULATION RESULTS OF A THREE-PHASE FAULT AT 3.45-KV BUS OF SYSTEM
WITH ORIGINAL SETTING

Voltage level	Fault voltage (p.u.)	Fault current (p.u.)	Relay operating time (t_{Ry})	Fault clearing time $\triangle t$
3.45 kV	0	9	0.312s	0.392s
11.4 kV	0.544	9	-	0.392s
33 kV	0.884	9	-	0.392s
161 kV	0.966	9	-	0.392s

TABLE V
ORIGINAL SETTINGS AND LIMITATION CONDITIONS

System parameter		Original setting	Limitation conditions
transformer	T_{r1}	161/33kV, 100MVA X_{T1}=12%	161/33kV, 100MVA 12%$<$$X_{T1}$$<$17%
	T_{r2}	33/11.4kV, 20MVA X_{T2}=10%	33/11.4kV, 20MVA 10%$<$$X_{T2}$$<$15%
	T_{r3}	11.4/3.45kV, 7.5MVA X_{T3}=6%	11.4/3.45kV, 7.5MVA 6%$<$$X_{T3}$$<$11%
relay	33kV CO-k_1	k_1=0.3	$0.21 \leqq k_1 \leqq 0.3$
	33kV LCO-k_{L1}	k_{L1}=0.3	$0.3 \leqq k_{L1} \leqq 0.39$
	11.4kV CO-k_2	k_2=0.2	$0.11 \leqq k_2 \leqq 0.2$
	11.4kV LCO-k_{L2}	k_{L2}=0.2	$0.2 \leqq k_{L2} \leqq 0.29$
	3.45kV CO-k_3	k_3=0.1	$0.01 \leqq k_3 \leqq 0.1$
	3.45kV LCO-k_{L3}	k_{L3}=0.1	$0.1 \leqq k_{L3} \leqq 0.19$

TABLE VI
CALCULATION VALUES USING HDE FOR A THREE-PHASE FAULT AT 3.45-KV
BUS

	X_{T1}	X_{T2}	X_{T3}	k_3
Case 1	0.9%	3.75%	6%	0.01
Case 2	0.9%	3.75%	10.5%	0.1
Case 3	0.9375%	5.0625%	10.5%	0.01

TABLE VII
CALCULATION RESULTS OF 11.4-KV BUS FOR A THREE-PHASE FAULT AT
3.45-KV BUS OF THE SYSTEM WITH HDE SOLUTION (t_{CB}=0.08s)

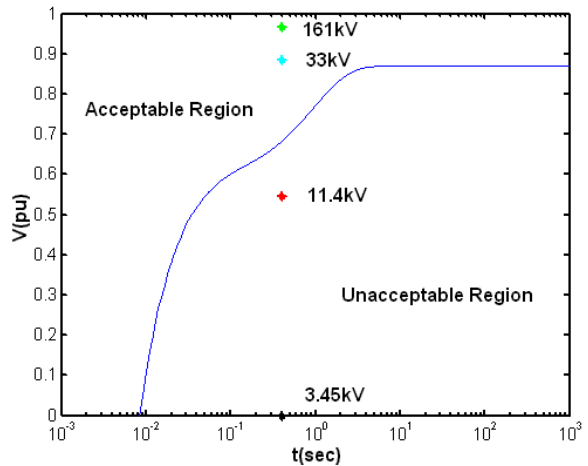|	Fault voltage (p.u.)	Fault current (p.u.)	Relay operating time (t_{Ry})	Fault clearing time	Objective function (p.u.)
Case 1	0.544	9	0.0311s	0.1111s	0.0622
Case 2	0.676	6.44	0.3688s	0.4488s	0.0147
Case 3	0.6222	5.9259	0.0386s	0.1186s	0

Fig. 7. Comparison of voltage sag and CBEMA curve for a three-phase fault at 3.45-kV bus and cleared after 0.392s of the system with original setting.
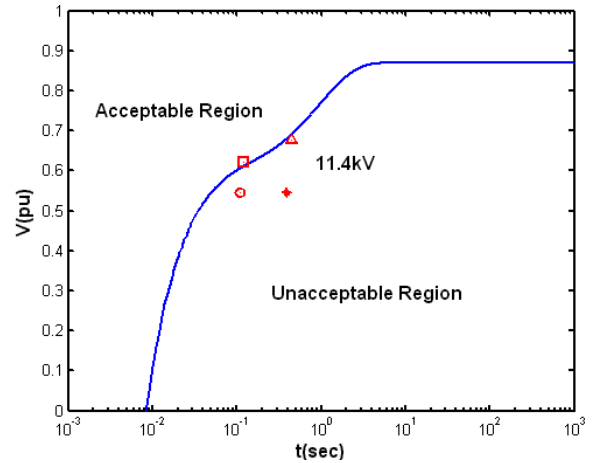

Fig. 8. Comparison of voltage sag and CBEMA curve of the 11.4kV for a three-phase fault at 3.45-kV bus of the system with HDE solution, (1)round: case 1, (2)triangle: case 2, (3)square: case 3.

(b)Single-line-ground fault

TABLE VIII shows the results of a single line-ground fault (SLG) at the 3.45-kV bus. The voltage sag range and duration of each voltage level are specified and compared with the CBEMA curve as plotted in Fig. 9 of the system with original settings. For the 11.4kV bus, the voltage is reduced to 0.7476 pu. The transformer impedances and LCO relay k values need be adjusted for three cases by HDE as shown in TABLE IX. TABLE X presents calculation results. The values of 11.4-kV bus are compared with the CBEMA curve as plotted in Fig. 10. The voltage sag has been improved.

TABLE VIII

SIMULATION RESULTS OF A SINGLE-LINE-GROUND FAULT AT 3.45-KV BUS OS SYSTEM WITH ORIGIAL ORIGINAL SETTING

Voltage level	Fault voltage (p.u.)	Fault current (p.u.)	Relay operating time (t_{Ry})	Fault clearing time $\triangle t = t_{Ry}+t_{CB}$ (t_{CB}=0.08s)
3.45 kV	0	10.69	0.2884s	0.3684s
11.4 kV	0.7476	10.69	-	0.3684s
33 kV	0.977	10.69	-	0.3684s
161 kV	1	10.69	-	0.3684s

TABLE IX

PARAMETER VALUES BY USING HDE OF A SINGLE-LINE-GROUND FAULT AT 3.45-KV BUS

	X_{T1}	X_{T2}	X_{T3}	k_{L3}
Case 1	0.9%	3.75%	6%	0.17
Case 2	0.9%	3.75%	10.5%	0.19
Case 3	0.9375%	5.0625%	10.5%	0.19

TABLE X

CALCULATION RESULTS OF 11.45-KV BUS OF A SINGLE-LINE-GROUND FAULT AT 3.45-KV BUS

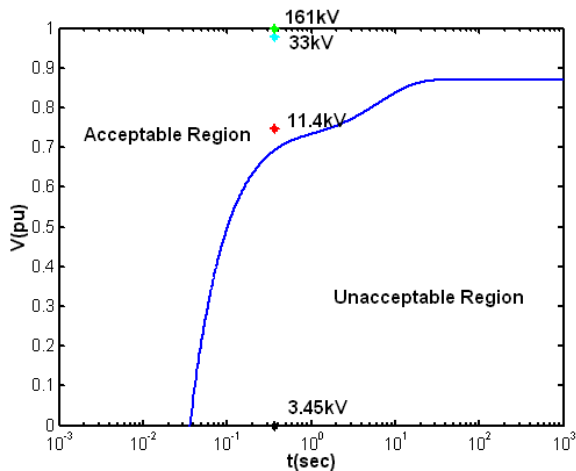|	Fault voltage (p.u.)	Fault current (p.u.)	Relay operating time (t_{Ry})	Fault clearing time	Objective function (p.u.)
Case 1	0.7476	6.175	0.4903s	0.5703s	0.0318
Case 2	0.8253	4.169	0.6596s	0.7396s	0.1005
Case 3	0.7938	3.914	0.6817s	0.7617s	0.0681

Fig. 9. Comparison of voltage sag and CBEMA curve for a single-line-ground fault (SLG, phase a) at 3.45-kV bus and cleared after 0.3684s of the system with original setting.
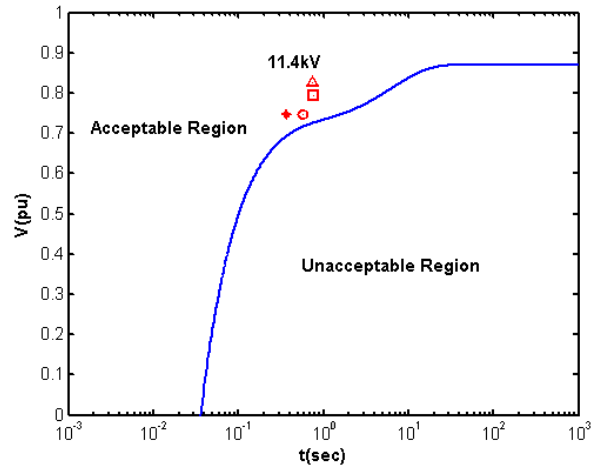

Fig. 10. Comparison of voltage sag and CBEMA curve of the 11.4kV side for a single-line-ground fault (SLG, phase a) at 3.45-kV bus of the system with HDE solution, (1)round: case 1, (2)triangle: case 2, (3)square: case 3.

(c)Consider margin of protective relay (HDE)

In order to consider the fault voltages and fault clearing times at all voltage levels, the protection time of upstream CO-relay is set 0.3 second later than downstream one[27-28], then $\triangle tk_2 = \triangle tk_3+0.3$, $\triangle tk_1 = \triangle tk_2+0.3$. When the 3.45-kV bus has a three-phase fault, the voltage and fault current are calculated as given in TABLE XI at every voltage level. Fig. 11 gives the voltage and relay clearing time of each voltage level. It can be found that the upstream 11.4-kV CO relay and the second upstream 33-kV CO relay satisfy the CBEMA curve in the acceptable area. If the upstream LCO-relay is also set 0.3 second later than the downstream one[27-28], then $\triangle tk_{L2} = \triangle tk_{L3}+0.3$, $\triangle tk_{L1} = \triangle tk_{L2}+0.3$. When the 3.45-kV bus has s single-line-ground fault, the voltage and fault current are given in TABLE XII at every voltage level. Fig. 12 displays the voltage and relay clearing time of each voltage level. It can be found that the upstream 11.4-kV LCO relay and the second upstream of 33-kV LCO relay satisfy the CBEMA curve in the acceptable area.

(d)Comparing with genetic algorithm

Figure 13 compares the efficiency and solution ability by using the HDE and a genetic algorithm (GA) to demonstrate the efficiency of the proposed method [27]. HDE and GA take 500 and 800 generations to converge, respectively. The computational burden of HDE is lighter because the population is smaller. The computational time is evaluated by the CPU time on a Pentium IV 1.6GHz computer as shown in TABLE XIII. It indicates that HDE is faster than GA. The value of the objective function obtained by HDE is better.
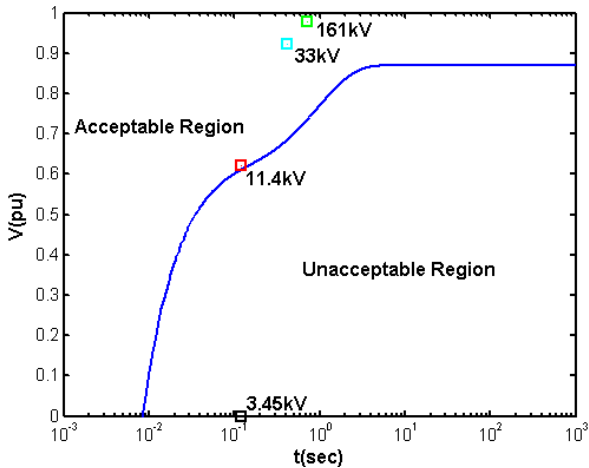
Fig. 11. Results of system with a three-phase fault at 3.45-kV bus, upstream CO relay with delay time, and with HDE solution (case 3).
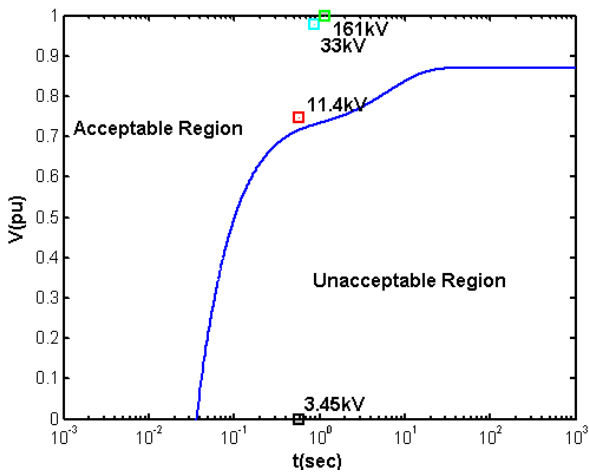

Fig. 12. Results of system with a single-line-ground fault at 3.45-kV bus, upstream LCO relay with delay time, and with HDE solution (case 1).
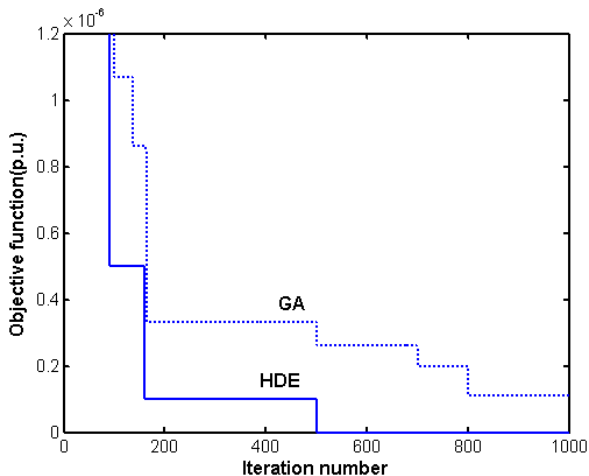

Fig. 13. Comparison of convergence between HDE and GA for three-phase fault (case 3).

TABLE XI
FAULT VOLTAGE, FAULT CURRENT, CO RELAY TIME-DELAY AND FAULT CLEARING TIME OF A THREE-PHASE FAULT AT 3.45-KV BUS WITH DELAY ON UPSTREAM CO RELAY AND HDE SOLUTION (CASE 3)

Voltage bus	Fault voltage (p.u.)	Fault current (p.u.)	Relay operating time (t_{Ry})	Fault clearing time $\triangle t = t_{Ry}+t_{CB}$ ($t_{CB}=0.08$s)
3.45kV	0	5.9259	0.0386s	0.1186s
11.4kV	0.6222	5.9259	0.3386s	0.4186s
33kV	0.9222	5.9259	0.6386s	0.7186s
161kV	0.9778	5.9259	-	-

TABLE XII
FAULT VOLTAGE, FAULT CURRENT, CO RELAY TIME-DELAY AND FAULT CLEARING TIME OF A SINGLE-LINE-GROUND FAULT AT 3.45-KV BUS WITH DELAY ON UPSTREAM LCO RELAY AND HDE SOLUTION (CASE 1)

Voltage rate	Fault voltage (p.u.)	Fault current (p.u.)	Relay operating time (t_{Ry})	Fault clearing time $\triangle t = t_{Ry}+t_{CB}$ ($t_{CB}=0.08$s)
3.45kV	0	6.175	0.4903s	0.5703s
11.4kV	0.7476		0.7903s	0.8703s
33kV	0.977		1.0903s	1.1703s
161kV	1		-	-

TABLE XIII
COMPARISON OF HDE AND GA FOR THREE-PHASE FAULT (CASE 3)

HDE		GA	
Objective function (p.u.)	0	Objective function (p.u.)	$0.11*10^{-6}$
N_P	5	N_P	70
CPU time (sec)	3.776	CPU time (sec)	80.6
C_R	0.5	Pc	0.8
F	0.01		
$\varepsilon 1$	0.1	Pm	0.05
$\varepsilon 2$	0.1		

VI. CONCLUSIONS

Through this study, the voltage sag severity can be controlled by adjusting the transformer impedance and relay setting. The settings of the protective relay and circuit breaker operating time determine the duration of voltage sag. In this paper, unbalanced short-circuit faults and unbalanced single-line-ground faults are used to investigate the problems of voltage sag. A systematic algorithm is used to obtain the voltage sag severity directly. So the optimization approach by using the HDE method is used to obtain the suitable transformer impedances and relay setting. The results are compared with the CBEMA curve. Simulation results show that the voltage sag can be improved by the proposed method.

REFERENCES

[1] M. H. J. Bollen, Understanding Power Quality Problems: Voltage Sags and Interruptions, IEEE, New-York, USA, 1999.

[2] IEEE Recommended Practice for Emergency and Standby Power Systems for Industrial and commercial Applications, IEEE Standard 446-1995, 1995.

[3] IEEE Recommended Practice for Powering and Grounding Electronic Equipment, IEEE Standard 1100-2005, 2006.

[4] IEEE Recommended Practice for Monitoring Electric Power Quality, IEEE Standard 1159-1995, 1995.

[5] J. C. Das, "Effects of Momentary Voltage Dips on the Operation of Induction and Synchronous Motors," IEEE Transactions on Industry Applications, Vol. 26, No. 4, pp. 711 -718, 1990.

[6] M. H. J. Bollen, "The Influence of Motor Reacceleration on Voltage Sags," IEEE Transactions on Industry Applications, Vol. 31, No. 4, pp. 667 -674, 1995.

[7] H. Shareef, A. Mohamed, and K. Mohamed, "Sensitivity of Compact Fluorescent Lamps during Voltage Sags: An Experimental Investigation", WSEAS Trans. on Power Systems, Vol. 5, No. 1, pp. 22-31, 2010.

[8] R. Ibrahim, A.M. A. Haidar, M. Zahim, H. Iu, "The Effect of DVR Location for Enhancing Voltage Sag", Proceedings of the 9th WSEAS International Conference on Application of Electrical Engineering, pp. 92-98, 2009.

[9] A. A. Koolaiyan, A. Sheikholeslami , R. A. Kordkheili, "A New Voltage Sag and Swell Compensator Switched by Hysteresis Voltage Control Method", Proceedings of the 8th WSEAS International Conference on Electric Power Systems, High Voltages, Electric Machines (POWER '08), pp. 71-76, 2008.

[10] Y. H.Chan and C. J. Wu, "Voltage Sag Analysis of Industry Power System Considering CBEMA Curve", Proceedings of the 10th WSEAS/IASME International Conference on Electric Power Systems, High Voltages, Electric Machines (POWER '10) pp. 107-111, 2010.

[11] C. T. Chi, "Dynamic Stability Analysis Based on Energy-Passivity Considerations", WSEAS Trans. on Circuits and Systems, Vol. 7, No. 3, pp. 119-128, 2008.

[12] M. H. J. Bollen, "Characterisation of Voltage Sags Experienced by Three-Phase Adjustable-Speed Drives," IEEE Transactions on Power Delivery, Vol. 12, No. 4, pp. 1666 -1671, 1997.

[13] G. Yalcinkaya, M. H. J. Bollen, and P. A. Crossley, "Characterization of Voltage Sags in Industrial Distribution Systems," IEEE Transactions on Industry Applications, Vol. 34, No. 4, pp. 682 -688, 1998.

[14] J. C. Gomez and M. M. Morcos, "Coordinating Overcurrent Protection and Voltage Sag in Distributed Generation System," IEEE Power Engineering Review, pp. 16-19, 2002.

[15] L. E. Conrad and M. H. J. Bollen, "Voltage Sag Coordination for Reliable Plant Operation," IEEE Transactions on Industry Applications, Vol. 33, No. 6, pp. 1459 -1464, 1997.

[16] J. Kyei, R. Ayanar, G. Heydt, and R. Thallam, "The Design of Power Acceptability Curves," IEEE Transactions on Power Delivery, Vol. 17, No. 3, pp. 828-833, 2002.

[17] G. T. Heydt, R. Ayyanar, R. Thallam, "Power Acceptability," IEEE Power Engineering Review, September 2001.

[18] J. C. Gomez and M. M. Morcos, "Voltage Sag and Recovery Time in Repetitive Events," IEEE Transactions on Power Delivery, Vol. 17, No. 4, pp. 1037-1043, 2002.

[19] G. J. Lee, M. M. Albu and G. T. Heydt, "A Power Quality Index Based on Equipment Sensitivity, Cost, and Network Vulnerability," IEEE Transactions on Power Delivery, Vol. 19, No. 3, pp. 1504-1510, 2004.

[20] G. T. Heydt and W. T. Jewell, "Pitfalls of Electric Power Quality Indices," IEEE Transactions on Power Delivery, Vol. 13, No. 2, pp. 570-578, 1998.

[21] Y. P. Chang and C. J. Wu, "Optimal Multi-objective Planning of Large-scale Passive Harmonic Filters Using Hybrid Differential Evolution Method Considering Parameter and Loading Uncertainty," IEEE Transactions on Power Delivery, Vol. 20, No. 1, pp. 408-416, 2005.

[22] J. P. Chiou and F. S. Wang, "A Hybrid Method of Differential Evolution with Application to Optimal Control Problems of a Bioprocess System," Proc. 1998 IEEE Conference on Evolutionary Computation, Vol. 1, pp. 627-632.

[23] F. S. Wang and H. J. Jang, "Parameter Estimation of A Bioreaction Model by Hybrid Differential Evolution," Proceedings of the 2000 Congress on Evolutionary Computation, Vol. pp. 410 − 417.

[24] Y. C. Lin, K. S. Hwang, and F. S. Wang, "Plant Scheduling and Planning Using Mixed-Integer Hybrid Differential Evolution with Multiplier Updating," Proceeding of IEEE Conference on Evolutionary Computation, Vol. 1, pp. 593-600, July 2000.

[25] Y. C. Lin, F. S. Wang, and K. S. Hwang, "A Hybrid Method of Evolutionary Algorithms for Mixed-Integer Optimization Problems," Proceeding of IEEE Conference on Evolutionary Computation, Vol. 3, pp. 2159-2166, July 1999.

[26] IEC Standard, Measuring relays and protection equipment, IEC 60255-22.

[27] A. Berizzi and C. Bovo, "The use of genetic algorithms for the localization and sizing of passive filters," Proceeding of the 9th International Conference On Harmonics and Quality of Power.

[28] P. M. Anderson, Power System Protection, IEEE Press Series on Power Engineering, Edition: 1, pp. 220-248, 1998.

Biographies

Yao-Hung Chan was born in Taiwan, 1969. He received the M. Sc. degree in electrical engineering from the Chang Gung University in 2001. Now he is studying for the Ph.D. degree in the National Taiwan University of Science and Technology. His research interests include electric power quality and power electronics.

Chi-Jui Wu received the B. Sc., M. Sc., and Ph.D. degree in electrical engineering all from the National Taiwan University in 1983, 1985, and 1988, respectively. In 1988, he joined the Department of Electrical Engineering, National Taiwan University of Science and Technology as an associate professor. Now he is a full professor. He has been active in practical problems and got many projects from private companies, independent research institutes, and governments. His current research interests lie in electric power quality, power electromagnetic interference, and power system stability.

Wei-Neng Chang was born in Tainan, 1963. He received the B. Sc., M. Sc., Ph.D. degree in electrical engineering from the National Taiwan University of Science and Technology in 1990, 1992, 1996. Currently, he is an Associate Professor in the Electrical Engineering Department, Chang Gung University, Taiwan. His research interests include microprocessor-based control system design, electric power quality and power electronics.

Ying-Pin Chang was born in Taiwan, 1965. He received the Ph.D. degree in electrical engineering from the National Taiwan University of Science and Technology in 2004. Currently, he is a professor in the Electrical Engineering Department at Nan Kai University of Science and Technology, Nantou, Taiwan. His research interests include electric power quality and power electronics.

Appendix: Hybrid Differential Evolution

A nonlinear constrained optimization problem can be expressed as

$$\text{Minimize } M(\underline{X}) \tag{A1}$$

where $M(\underline{X})$:objective function of variable vector $\underline{X}$,

$$\underline{X} = \left[X_1, X_2, ..., X_j, ..., X_D \right]^t$$

The DE is a parallel direct search method for minimizing nonlinear and non-differential objective functions. The fitness of an offspring is determined by one-to-one competition with the corresponding parent. The solution procedures are given as follows.

(1)Initialization: The initial populations $\underline{X}_i^0, i=1,2,...,N_P$ are chosen randomly and should cover the entire search space uniformly. The elements of individual $\underline{X}_i^0$ are given by

$$X_{ji}^0 = X_j^{min} + \rho_i (X_j^{max} - X_j^{min}),$$
$$j=1,2,...,D \ , i=1,2,...,N_p \tag{A2}$$

where $\rho_i \in [0,1]$ is a random number, and N_P is the population size. X_j^{min} and X_j^{max} are the lower and upper bounds of the respective variable.

(2)Mutation operation: At generation G, a mutant vector is generated based on the present individual $\underline{X}_i^G$ by

$$\underline{U}_i^{G+1} = \underline{X}_i^G + F(\underline{X}_{r1}^G - \underline{X}_{r2}^G), \ i=1,2,...,N_p \tag{A3}$$

where $i \neq r1, i \neq r2$, and $r1,r2 \in \{1,2,...N_P\}$. $F \in [0,1]$ is a scalar factor. $\underline{X}_{r1}^G$ and $\underline{X}_{r2}^G$ are two randomly selected individuals.

(3)Crossover operation: To extend the diversity of individuals in the next generation, the perturbed

individual $\underline{U}_i^{G+1} = \left[U_{1i}^{G+1}, U_{2i}^{G+1}, ..., U_{ji}^{G+1}, ..., U_{Di}^{G+1} \right]^t$ and the present

individual $\underline{X}_i^G = \left[X_{1i}^G, X_{2i}^G, ..., X_{ji}^G, ..., X_{Di}^G \right]^t$ are mixed to yield the trial vector

$$\underline{\hat{U}}_i^{G+1} = \left[\hat{U}_{1i}^{G+1}, \hat{U}_{2i}^{G+1}, ..., \hat{U}_{ji}^{G+1}, ..., \hat{U}_{Di}^{G+1} \right]^t \tag{A4}$$

where

$$\hat{U}_{ji}^{G+1} = \begin{cases} X_{ji}^G, \text{if a random number} > C_R \\ U_{ji}^{G+1}, \text{otherwise} \end{cases}$$
$$j=1,2,...,D , i=1,2,...,N_P \tag{A5}$$

where D is also the number of genes. $C_R \in [0,1]$ is the crossover factor and must be set by the user.

(4)Evaluation and selection: The parent is replaced by its offspring in the next generation if the fitness of the later is better. Contrarily, the parent is retained. The first step is one-to-one competition. The next step selects the best individual, $\underline{X}_b^{G+1}$ in the population. That is

$$\underline{X}_i^{G+1} = arg\text{-}min\{M(\underline{X}_i^G), M(\underline{\hat{U}}_i^{G+1})\},$$
$$i=1,2,...,N_P \tag{A6}$$

$$\underline{X}_b^{G+1} = arg\text{-}min\{M(\underline{X}_i^{G+1})\},$$
$$i=1,2,...,N_P \tag{A7}$$

where *arg-min* means the argument of the minimums.

The above steps are repeated until the maximum iteration number or the desired fitness is achieved. In general, faster descent usually leads to a local minimum or a premature convergence. Conversely, the diversity guarantees a high probability of obtaining the global optimum. The trade-off can be achieved by slightly lowering the scaling factor *F* and by increasing the population size N_P. However, more computation time is required. The migrant and accelerated operations in HDE are used to overcome the local minimum solution and time consumption. The migrant and accelerating operations are embedded in the original DE.

(5)Migrant operation if necessary: To increase search space exploration, a migration operation is introduced to regenerate a diverse population of individuals. The migrant individuals are chosen on a "best individual" basis $\underline{X}_b^{G+1}$. The jth gene of $\underline{X}_i$ is regenerated by

$$X_{ji}^{G+1} = \begin{cases} X_{jb}^{G+1} + \rho_1(X_j^{min} - X_{jb}^{G+1}), & \text{if } \rho_2 < \dfrac{X_{jb}^{G+1} - X_j^{min}}{X_j^{max} - X_j^{min}} \\ X_{jb}^{G+1} + \rho_1(X_j^{max} - X_{jb}^{G+1}), & \text{otherwise} \end{cases} \tag{A8}$$

Where ρ_1 and ρ_2 are randomly generated numbers uniformly distributed in [0,1]. The migrant population will not only

become a set of newly promising solutions, but also avoid the local minimum trap.

The migrant operation is performed only if a measure fails to match the desired population diversity tolerance. The measure in this study is defined as

$$u = \frac{\left[\displaystyle\sum_{\substack{i=1 \\ i \neq b}}^{N_P} \sum_{j=1}^{D} \eta_{ji}\right]}{D(N_P - 1)} < \varepsilon_1 \qquad (A9)$$

where

$$\eta_{ji} = \begin{cases} 1, & \text{if } \left|\dfrac{X_{ji}^{G+1} - X_{jb}^{G+1}}{X_{jb}^{G+1}}\right| > \varepsilon_2 \\ 0, & \text{otherwise} \end{cases} \qquad (A10)$$

Parameters $\varepsilon_1 \in [0,1]$ and $\varepsilon_2 \in [0,1]$ express the desired tolerance of the population diversity and the gene diversity with regard to the best individual, respectively. Here η_{ji} is defined as an index of the gene diversity. A zero η_{ji} means that the jth gene of the ith individual is close to the jth gene of the best individual. If the degree of population diversity u is smaller than ε_1, the HDE performs migration to generate a new population to escape the local point. Otherwise, HDE breaks off the migration, which maintains an ordinary search direction.

(6)Accelerated operation if necessary: When the fitness in the present generation is not improved any longer using the mutation and crossover operations, a descent method is then applied to push the present best individual toward a better point. Thus, the acceleration operation can be expressed as

$$\hat{\underline{X}}_b^{G+1} = \begin{cases} \underline{X}_b^{G+1}, & \text{if } M(\underline{X}_b^{G+1}) < M(\underline{X}_b^G) \\ \underline{X}_b^{G+1} - \alpha \nabla M(\underline{X}_b^{G+1}), & \text{otherwise} \end{cases} \qquad (A11)$$

The gradient of the objective function, $\nabla M(\underline{X}_b^{G+1})$, can be calculated approximately with finite difference. The step size $\alpha \in (0,1]$ is determined according to the decent property. Firstly, α is set to unity. The objective function $M(\hat{\underline{X}}_b^{G+1})$ is then compared with $M(\underline{X}_b^{G+1})$. If the decent property is achieved, $\hat{\underline{X}}_b^{G+1}$ becomes a candidate in the next generation, and is added into this population to replace the worst individual. On the other hand, if the decent requirement fails, the step size is reduced, for example, 0.5 or 0.7. The decent search method is repeated to find the optimal $\hat{\underline{X}}_b^{G+1}$, called $\underline{X}_b^N$, at the $(G+1)^{th}$ generation. This result shows the objective function $M(\underline{X}_b^N)$ should be at least equal or smaller than $M(\underline{X}_b^{G+1})$.